

Novel cofactors via post-translational modifications of enzyme active sites

Nicole M Okeley and Wilfred A van der Donk

Recent crystallographic and biochemical studies have revealed the existence of numerous novel post-translational modifications within enzyme active sites. These modifications create structural and functional diversity. Although the function and biosynthesis of some of these modifications are well understood, others need further investigation.

Address: Department of Chemistry, University of Illinois at Urbana-Champaign, Urbana, IL 61801, USA

Correspondence: Wilfred A van der Donk
E-mail: vddonk@uiuc.edu

Chemistry & Biology 2000, 7:R159–R171

1074-5521/00/\$ – see front matter
© 2000 Elsevier Science Ltd. All rights reserved.

Introduction

The catalytic power of enzymes has long intrigued chemists and biologists alike. Many enzymes utilize low molecular weight organic cofactors for catalysis, some of which are covalently linked to the protein. For the most part, these cofactors, such as hemes or flavins, are non-proteinaceous and are independently biosynthesized before their introduction into the protein. In recent years, the increasing availability of structural information has revealed a growing number of enzymes that have evolved an alternative means for generating cofactors. This alternative route relies on the post-translational processing of encoded residues to form novel structural motifs in the protein's active site. Many of these modifications were unanticipated prior to their structural elucidation, and have forced a re-evaluation of the catalytic mechanisms of the enzymes in question. In addition, the discovery of these novel cofactors has led to much interest in the mechanisms of their biosynthesis. This review will focus on the novel structures that have been characterized by biochemical and crystallographic studies (Figure 1), and their proposed roles in catalysis.

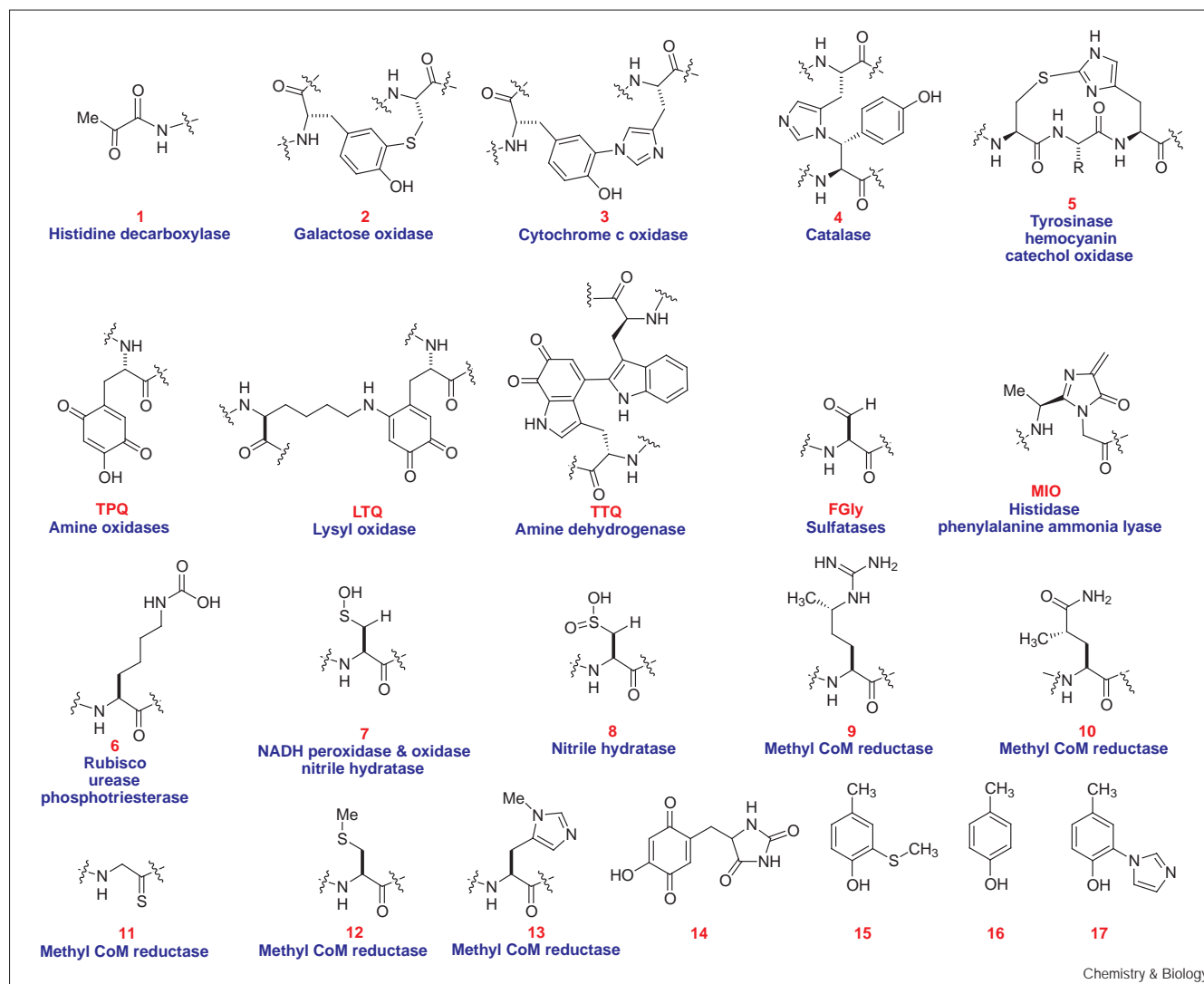
Histidine decarboxylase/D-proline reductase

Historically, histidine decarboxylase was one of the first enzymes reported to undergo post-translational modification of one of its encoded amino acids to generate a cofactor. Amino acid decarboxylases typically contain pyridoxal 5'-phosphate (PLP) as an essential coenzyme. Snell and coworkers [1] demonstrated, however, that histidine decarboxylase from *Lactobacillus 30a* does not utilize PLP, but instead contains a different reactive carbonyl functionality. Further experiments revealed the presence of a covalently bound amino-terminal pyruvoyl group (1) that was derived from an encoded serine residue [1]. Several other pyruvoyl-dependent decarboxylases have been identified since [1], including D-proline [2] and L-glycine reductase [3]. The role of the pyruvoyl cofactors is to form a Schiff base with substrate during catalysis to facilitate decarboxylation. Histidine decarboxylase catalyzes the decarboxylation of histidine to histamine (Figure 2). It is composed of two subunits (α and β) that originate from the autocatalytic cleavage of an inactive pro-enzyme. This process generates the pyruvoyl group via a nonhydrolytic serinolysis. Snell and coworkers [1] have shown that the pyruvoyl group on the amino terminus of the α subunit arises from Ser82 of the pro-enzyme, whereas the serine on the carboxyl terminus of the β subunit arises from Ser81 (Figure 3).

Quinoproteins

Long before the actual identification of their cofactors, copper-dependent amine oxidases and bacterial amine

Figure 1



The structural diversity created by the post-translational modifications discussed in this review are shown, as well as some model compounds that have been studied to understand the physicochemical or catalytic properties of some of these novel cofactors. Compound 14 catalyzes amine oxidation and has contributed to understanding of

TPQ-dependent enzymes [13]. Compounds 15–17 have been used to probe the modulation of pK_a and redox potential of phenols when substituted with a thioether as in galactose oxidase [29], or with imidazole [36], as in cytochrome c oxidase.

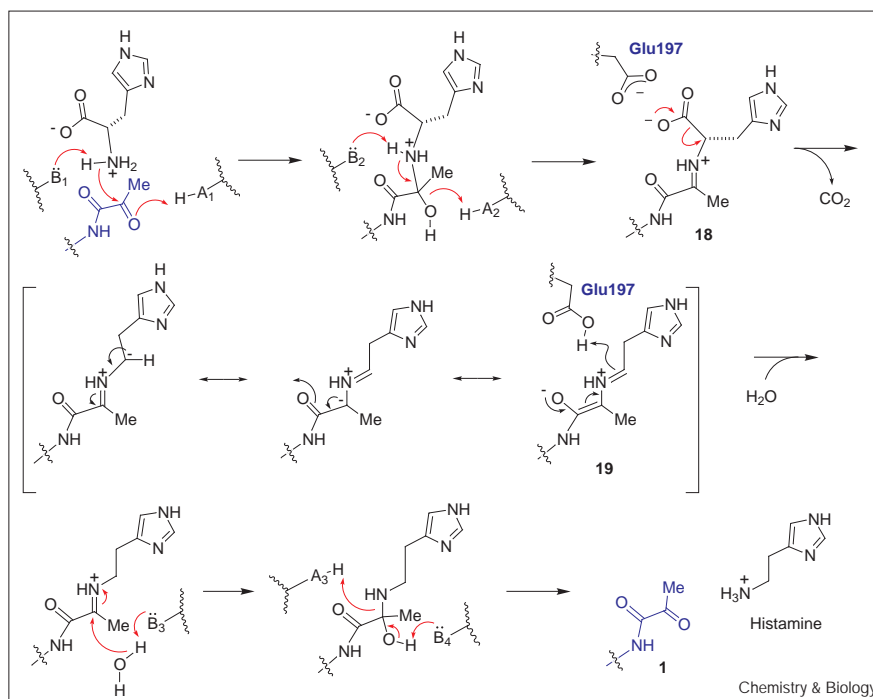
dehydrogenases were suspected to contain a covalently bound reactive carbonyl group. Initial studies led to suggestions that the prosthetic groups might consist of a bound pyridoxal derivative or pyrroloquinoline quinone (PQQ), two exogenous cofactors. More recently, it has been shown that, in fact, three novel post-translationally derived quinone cofactors are present in these proteins (Figure 1) [4]. In a series of impressive biochemical studies, Klinman and coworkers [5] established the structure of 2,4,5-trihydroxyphenylalanine quinone (TPQ or TOPA quinone). Subsequently, McIntire, Lidstrom and coworkers [6] identified tryptophan tryptophylquinone (TTQ) in methylamine dehydrogenase (MADH), and

Klinman, Dooley and coworkers [7] ascertained the identity of lysine tyrosylquinone (LTQ) in mammalian lysyl oxidase. More recently, the structures of TPQ [8–10] and TTQ [11] have been confirmed unambiguously by crystallography. The following sections will discuss the current understanding of the biogenesis of these cofactors and their roles in catalysis.

Copper-dependent amine oxidases: modification of tyrosine
Copper-containing amine oxidases catalyze the two-electron oxidation of primary amines to their corresponding aldehydes. These enzymes are ubiquitous in Nature and display strong diversity in substrate structure and physiological

Figure 2

Proposed catalytic cycle for histidine decarboxylase [1]. The exact identity of the various acid–base catalysts (A_nH , B_n) has not been unambiguously established. The amine of the substrate forms a Schiff base 18 with the carbonyl of the amino-terminal pyruvoyl group (shown in blue). The active site crystal structure [72] and the enzyme's pH optimum suggest that the decarboxylation step is favored by the orientation of the carboxyl group of the substrate and Glu197, which could provide electrostatic destabilization to promote decarboxylation. The structures in brackets are resonance forms of the delocalized anion 19, which may be protonated by Glu197. The catalytic cycle is completed by hydrolysis of the Schiff base, liberating histamine and the free pyruvoyl group.



roles, ranging from histamine oxidation and cell signaling in animals to secondary metabolism and programmed cell death in plants. The catalytic cycle consists of a reductive half-reaction, in which the substrate amine is oxidized and the TPQ cofactor is reduced to the aminoquinol form, followed by an oxidative half-reaction in which the aminoquinol is re-oxidized to TPQ by O_2 , releasing NH_3 and H_2O_2 (Figure 4).

Although the mechanism of the reductive half-reaction has been extensively studied and is generally agreed upon (steps 1–3, Figure 4), the details for the oxidative half-reaction are less well-understood, and recently the

dogma that copper is essential as a redox partner has become a point of contention. At present, two different models have been put forward. In the original mechanism, internal electron transfer from the aminoquinol to $Cu(II)$ generates a $Cu(I)$ /aminosemiquinone form of the enzyme (step 4, Figure 4). Oxygen subsequently reacts with the $Cu(I)$ center, followed by a second electron transfer from the amino-semiquinone to the copper-bound superoxide. In contrast, the second more recent model proposes direct electron transfer from reduced aminoquinol to O_2 (step 5A) [12]. In this mechanism, the $Cu(I)$ -semiquinone is not an intermediate and the copper fulfills merely an electrostatic role during

Figure 3

Proposed mechanism of biogenesis of the pyruvoyl cofactor [1]. Ser82 attacks the carbonyl of Ser81, followed by collapse of the tetrahedral intermediate to generate 20. Subsequent elimination releases the β subunit and produces dehydroalanine 21, which is hydrolyzed to provide the pyruvoyl moiety at the amino terminus of the α subunit. The oxygen atom of Ser82 (red) ends up in the carboxy-terminal carboxylate of the β chain [1].

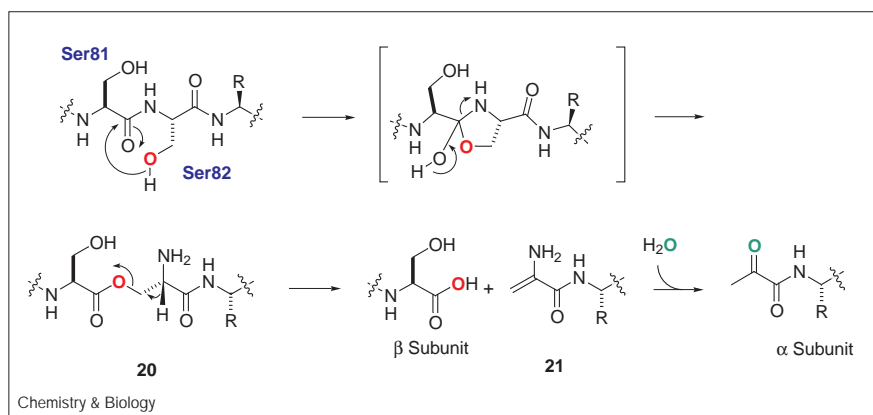
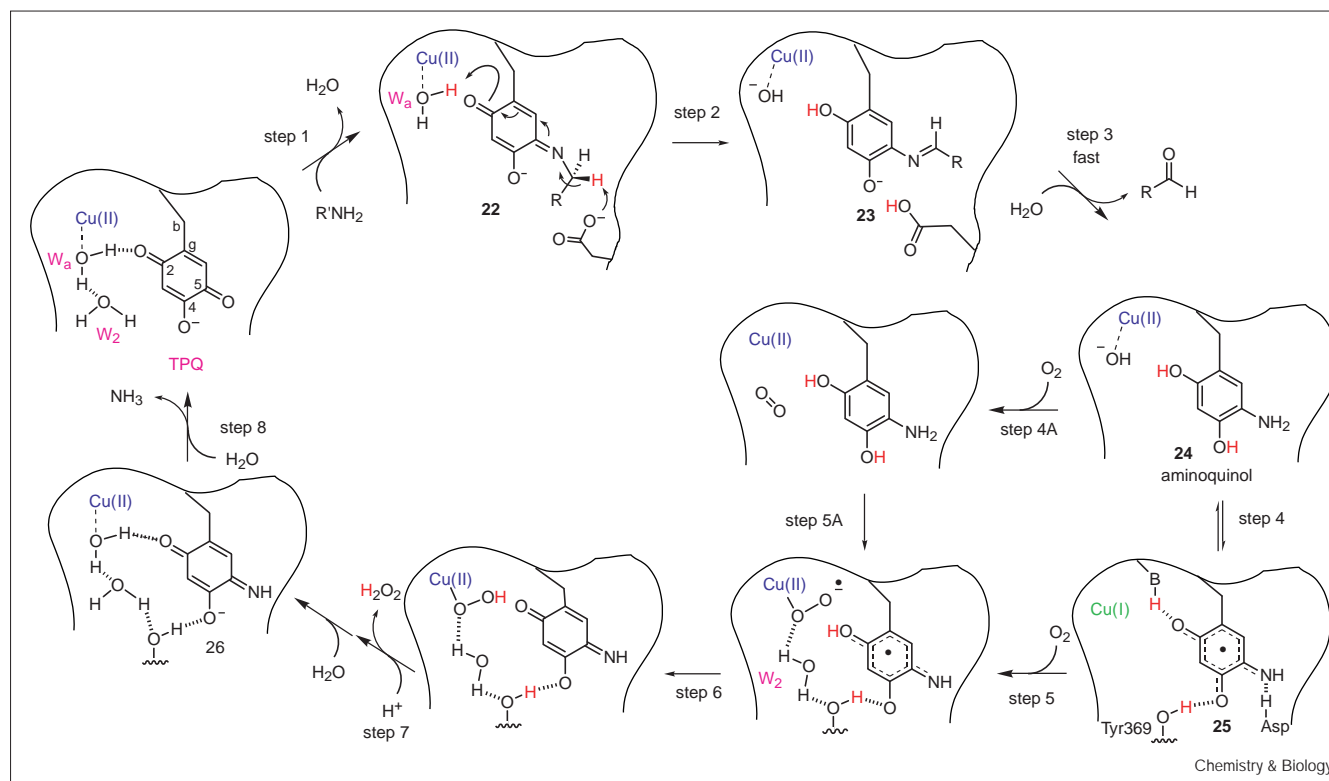


Figure 4



Proposed catalytic cycle of amine oxidases. Steps 1–3 comprise the reductive half-reaction. Initially a Schiff base complex (22) is formed at C5 of the cofactor. Deprotonation of the complex by a strictly conserved aspartate residue produces a new Schiff base (23). Hydrolysis generates the aldehyde product and aminoquinol (24). The two additional protons on the reduced cofactor shown in red have been postulated to originate from the substrate via the catalytic base, and from a copper bound water [12,15]. One of the proposed mechanisms for the oxidative half-reaction involves initial electron transfer from the aminoquinol to copper generating a Cu(I)-amino

semiquinone (25). Both forms (24 and 25) have been observed under certain conditions suggesting they may be in equilibrium [73,74]. Reaction of Cu(I) with O_2 generates a copper bound superoxide. A second electron and proton transfer generates H_2O_2 and iminoquinone 26 that is either hydrolyzed to release ammonia and regenerate TPQ or reacts directly with another amine substrate to enter the reductive half-reaction as 22. The two protons in the hydrogen peroxide product ultimately originate from substrate and copper-bound water. In the second mechanism, Cu(I) is not involved and electron transfer occurs directly from aminoquinol to molecular oxygen (step 5A).

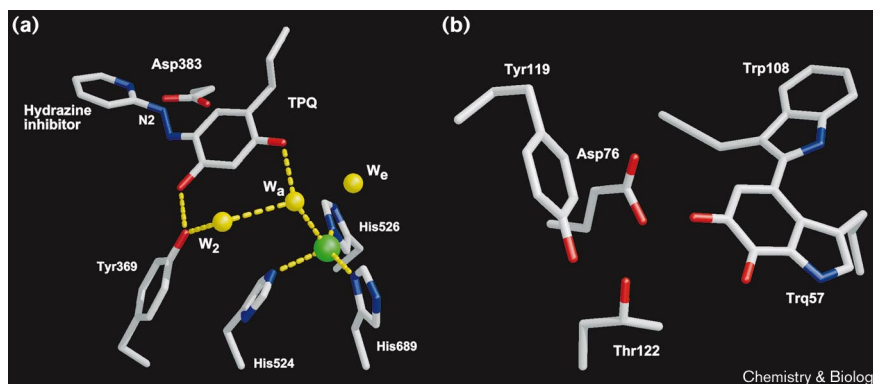
turnover, stabilizing or coordinating the anionic superoxide and hydroperoxide intermediates. Support for this unconventional model is provided by kinetic studies indicating that O_2 binding and the first electron transfer to O_2 are separate events, which is inconsistent with binding of O_2 to Cu(I). Instead, this suggests O_2 binding occurs at a site other than copper (step 4A) [12]. Direct reduction of oxygen by aminoquinols has precedent in model studies on hydantoin 14 (Figure 1), which is able to catalytically oxidize primary amines to aldehydes in the absence of copper [13]. In addition, several reports have suggested that non-redox-active metals can substitute for copper [14] (J.P. Klinman and S. Mills, personal communication), consistent with an electrostatic function, but not with a redox-active role for copper.

The structures of amine oxidases from several different species have been reported in the past five years [8–10].

Comparison of the orientation of TPQ in the various structures suggests that it can rotate 180° about its C β –C γ bond, and that it is not coordinated to copper in active enzyme crystals. Only in the structure from *Hansenula polymorpha* [10] and the *Escherichia coli* enzyme inactivated with a hydrazine inhibitor (Figure 5a) [8] is the TPQ residue oriented in a position compatible with catalysis. In this orientation, O4 is engaged in a strong hydrogen bond with the phenol of Tyr369, and O5 is close to a conserved aspartate, the proposed active site base. Very recently, three intriguing structures of enzyme intermediates in the oxidative half-reaction have been determined using flash-freezing techniques [15]. One of the structures contains a dioxygen molecule, probably hydrogen peroxide, bound to copper. In this structure, the two proposed proton transfer networks in Figure 4 that transport the protons from O2 and O4 of the aminoquinol to molecular oxygen can be visualized.

Figure 5

(a) *E. coli* amine oxidase with a 2-hydrazinopyridine inhibitor bound to C5 of TPQ [8] (PDB code 1SPU). Asp383 is close to N2 of the inhibitor, consistent with it being the catalytic base that deprotonates the substrate Schiff base complex 22 (Figure 4). Copper (green) is coordinated by three histidine residues and two waters (yellow) in a distorted square pyramidal geometry. The apical water ligand (Wa) hydrogen bonds to O2 of TPQ, and forms an additional hydrogen bond to another water (W2), which is hydrogen bonded to a conserved tyrosine residue [15]. This Tyr369 is in turn hydrogen bonded to O4 of TPQ. A third water, which is present as an equatorial ligand in apo-enzyme (Cu-O, 2.0 Å), is at a distance of 3.0 Å from the copper. (b) The active site of methylamine dehydrogenase from *Paracoccus denitrificans* (PDB code 2BBK) [75]. The two indole rings



of TPQ are non-coplanar and make a dihedral angle of about 42°. Interestingly, in the X-ray structure of the ternary complex between MADH, amicyanin and cytochrome c-551i, the

terminal electron acceptor, the indole moiety of Trp108 in MADH is oriented towards the copper site of amicyanin at a distance of 9.4 Å [22]. Trq, tryptophylquinone.

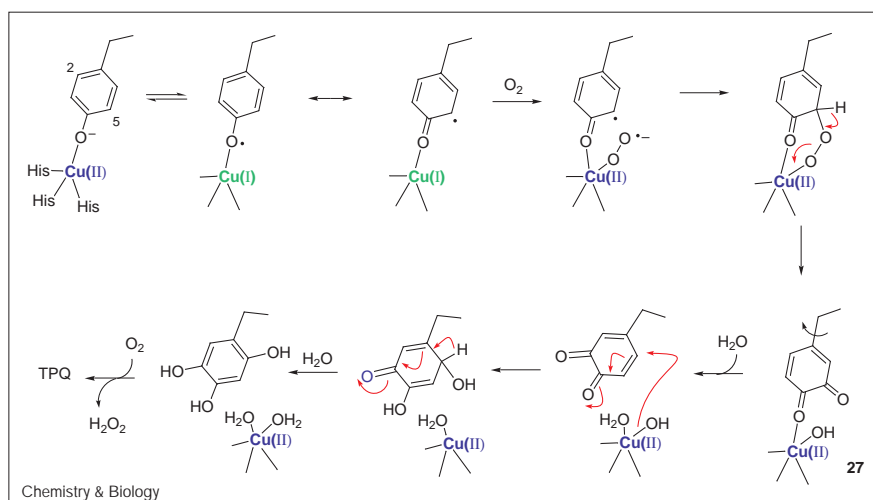
The TPQ cofactor is found within the highly conserved peptide -TXXNY(D/E)Y (single-letter amino-acid code) in which the strictly conserved first tyrosine residue is modified to TPQ. Two independent studies provided the first evidence for a self-catalytic post-translational oxidation [16,17]. The enzyme from *A. globiformis* has been expressed in *E. coli* in the copper-free apo-form in which the tyrosine residue has not been processed [16]. This has allowed detailed studies of the autocatalytic generation of TPQ. Ruggiero and Dooley [18] have shown recently that TPQ formation consumes two molecules of O₂, producing one molecule of H₂O₂. On the basis of the position of the tyrosine residue in the structure of the apo-protein [9], a mechanism for TPQ biogenesis has been proposed in which the tyrosine is initially coordinated to the copper (Figure 6) [19].

Lysyl oxidase: a modified tyrosine cross-linked to lysine

Lysyl oxidase catalyzes the post-translational formation of cross-links in elastin and collagen during the formation of connective tissue. Mammalian lysyl oxidase contains copper and shows characteristics very similar to other members of the amine oxidase enzyme family. It does, however, lack the TPQ consensus sequence, and recent studies have revealed the cofactor to be a variation of TPQ in which a lysine residue is linked to a modified tyrosine residue to produce LTQ (Figure 1). At present, no structural information is available for the enzyme, and no studies on the mechanism of biogenesis of LTQ have been reported. Several biosynthetic pathways have been proposed that share a common ortho-quinone intermediate (27, Figure 6) with the proposed

Figure 6

Proposed mechanism of biogenesis of TPQ [19]. Electron transfer from the tyrosinate to Cu(II) generates a Cu(I)-tyrosyl radical. Molecular oxygen is reduced by Cu(I) to superoxide, which reacts with the tyrosyl radical at C5. Fragmentation of the copper-bound peroxide leads to a cupric hydroxide and orthoquinone 27, which rotates 180° around its Cβ-Cγ bond. Michael addition of hydroxide to the quinone followed by aromatization gives 2,4,5-trihydroxyphenylalanine, which is oxidized by a second molecule of O₂ to form TPQ and H₂O₂.



pathway of TPQ formation [7]. Addition of lysine to this intermediate instead of hydroxide would produce LTQ. It is interesting to note that the nonmammalian lysyl oxidase from *Pichia pastoris* does not contain LTQ but rather TPQ, consistent with the presence of the TPQ consensus sequence [20].

In addition to LTQ, another variant on the tyrosine-derived quinone theme has been reported recently in an amine oxidase from *Aspergillus niger*, which contains an ester linkage at position 2 of the quinone to the γ -carboxylate of a glutamate [21]. Whether this structure was produced during the isolation of a phenylhydrazone-labeled peptide or is present in the native enzyme remains to be established. It is currently unclear what the basis is for the evolution of the various quinone structures. As model compounds for the reduced forms of TPQ, LTQ and PQQ all have similar oxidation potentials, it appears that differences in the reductive half-reactions have provided the evolutionary pressure that has led to these different structures [7].

Methylamine dehydrogenase: a modified Trp–Trp cross-link

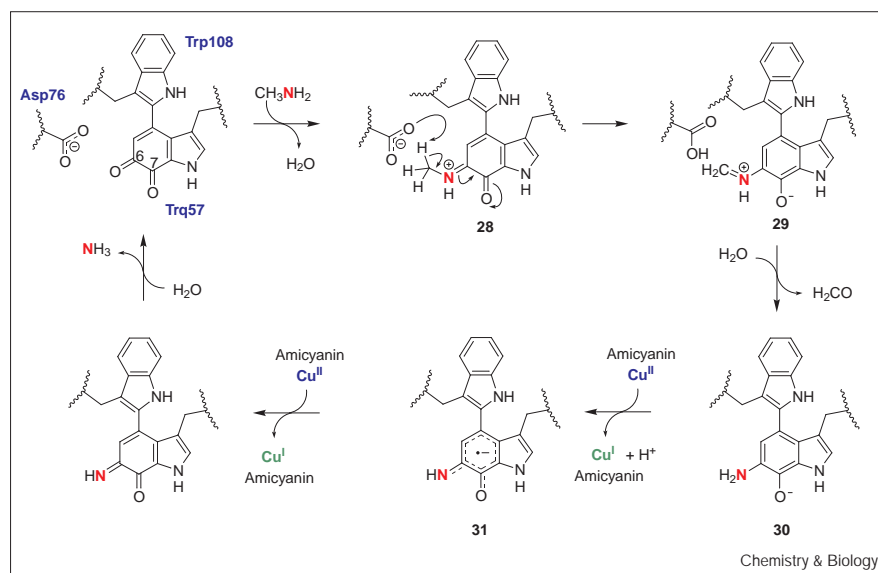
Methylamine dehydrogenases (MADH) from various methylotrophic bacteria catalyze the deaminative oxidation of methylamine to formaldehyde and ammonia. Like the amine oxidases discussed in the previous section, methylamine dehydrogenases utilize an amino-acid-derived quinone cofactor for catalysis. Isolation of a peptide containing the semicarbazide derivatized cofactor allowed the identification of its structure as two cross-linked tryptophans (Figure 5b) [6]. A re-evaluation of crystallographic data collected earlier confirmed the proposed structure [11]. The mechanism of the oxidation of amine to aldehyde in methylamine dehydrogenase (Figure 7) is similar to the

reductive half-reaction catalyzed by the copper amine oxidases (steps 1–3, Figure 4). The reoxidation of the cofactor, however, does not require O_2 but instead involves two consecutive one-electron transfer steps from reduced TTQ to the copper protein amicyanin in its Cu(II) oxidation state [22]. Genetic analysis suggests that biosynthesis of TTQ is not an autocatalytic event as for TPQ, but requires at least two gene products: MauG, a protein with sequence similarity to a cytochrome *c* peroxidase from *Pseudomonas* sp., and MauL with no known homology to any proteins in the protein databases. MauG is thought to be involved in the cross-linking of tryptophylquinone (Trq) 57 and Trp108 (see [23] for references).

Galactose oxidase: a Tyr–Cys cross-link

The extracellular fungal protein galactose oxidase catalyzes the oxidation of a broad range of alcohols, including galactose, to their corresponding aldehydes concomitant with reduction of O_2 to H_2O_2 , the biologically relevant product. The hydrogen peroxide is subsequently used as co-substrate for peroxidases and/or as bacteriostatic agent. There has been much speculation regarding how the single copper center in the protein can achieve a two-electron oxidation [23,24]. In the late 1980s Whittaker and Whittaker [25] proposed that the two oxidizing equivalents are stored in the form of a protein radical that is electronically coupled to a copper(II) ion. This proposal was supported by the observation that the active state of the enzyme did not display a copper(II) electron paramagnetic resonance (EPR) signal, even though X-ray absorption near edge spectroscopy (XANES) indicated that the enzyme actually did contain copper(II) [24]. Indeed, later studies succeeded in producing and characterizing a protein radical in copper-free apo-enzyme, which was

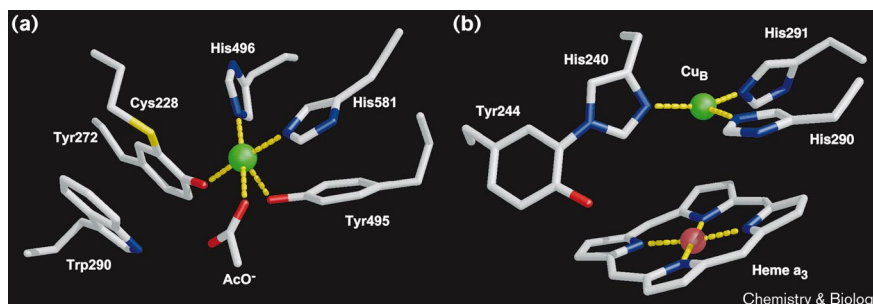
Figure 7



Proposed mechanism for methylamine dehydrogenase [76]. The amine substrate forms a Schiff base (28) at C6 of TTQ, followed by deprotonation of the substrate by a general base thought to be Asp76 (Figure 5b). This leads to formation of a new Schiff base 29. Hydrolysis of the iminium generates an aminoquinol (30) and formaldehyde. Zhu and Davidson [76] have provided evidence that an N-semiquinone radical 31 is formed in the first step of the oxidative half reaction. A second electron transfer produces the iminoquinone, which is hydrolyzed to release ammonia.

Figure 8

(a) Active-site structure of galactose oxidase from crystals obtained at pH 4.5 (PDB code 1GOF) [27]. The copper coordination geometry is square pyramidal with two histidine residues, acetate (water in structures at pH 7), and the phenol oxygen of the Tyr–Cys cross-link forming the basal plane, and the conserved Tyr495 as the axial ligand. (b) The binuclear center of cytochrome c oxidase from bovine heart in the reduced state (PDB code 1OCR) [33]. The axial histidine ligand to the heme (His) and the heme sidechains are omitted for clarity. Tyr244 is positioned such that it could provide a hydrogen bond to the distal oxygen atom of molecular oxygen coordinated to the heme (Figure 10).



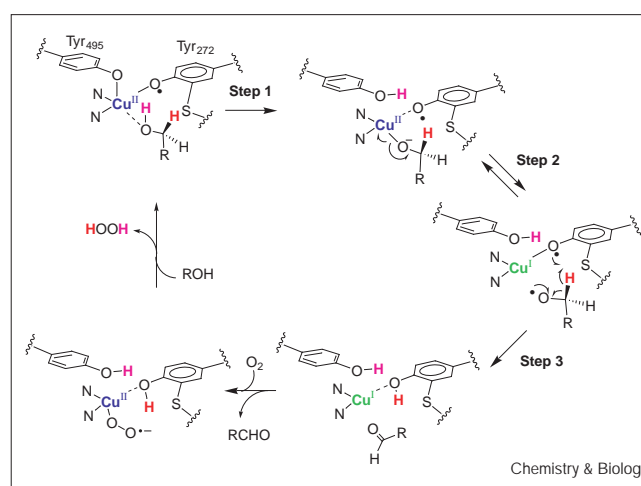
shown to be associated with a tyrosine residue [26]. When the crystal structure of the enzyme was determined, an unanticipated post-translational modification of Tyr272 was revealed [27]. This residue is covalently linked at Cε to the sulfur of Cys228 (Figure 8a). Spectroscopic and model studies have now conclusively shown that this residue is the radical site in apo-enzyme [24], and it is generally believed that this radical is electronically coupled to Cu(II) in the holo-enzyme, thereby prohibiting its detection by EPR for many decades.

The most recently proposed mechanism for catalysis is shown in Figure 9 [24]. Similar to the amine oxidases and dehydrogenase described above, the catalytic cycle can be divided into reductive (steps 1–3) and oxidative half-reactions. The functional role of the Tyr–Cys cross-link in this mechanism has been investigated in both protein and model studies. The one-electron redox potential for oxidation of Cu(II)-tyrosinate to Cu(II)-tyrosyl radical in the protein is decreased by a remarkable 500 mV (~11 kcal mol⁻¹) or more [28] compared with tyrosine residues in other proteins [23]. A similar, albeit less dramatic, lowering of the oxidation potential is observed in the model compound 15 (Figure 1) [29]. It appears, therefore, that the functional role of the thioether cross-link is to promote one-electron chemistry as opposed to the two-electron redox processes catalyzed by the quinone cofactors discussed above.

The thioether substitution also lowers the pK_a of the phenol of 15 by about 0.6 compared with p-cresol (16) (Figure 1) [29]. Combining the experimentally determined values of the equilibrium acidities (pK_a) and oxidation potential for the conjugate anions of 15 and p-cresol allows an estimation of the influence of the thioether on the bond dissociation energy (BDE) of the oxygen–hydrogen bond using a thermodynamic cycle. This calculation indicates that introduction of the covalent carbon–sulfur linkage

decreases the BDE by ~3.6 kcal mol⁻¹. This lowering suggests that, from a thermodynamic perspective, hydrogen atom abstraction from substrate in step 3 of the reductive half-reaction is altered unfavorably by the thioether linkage. The reduced redox potential of the cross-link, however, facilitates radical formation in the oxidative half-reaction. The Tyr–Cys cross-link is not limited to galactose oxidase and is also found in several other oxidases [24]. At present, little is known about the mechanism of its formation.

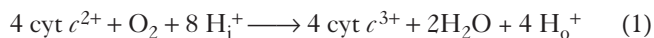
Figure 9



Proposed catalytic cycle for galactose oxidase [24]. The reductive half reaction is shown in steps 1–3; the oxidative half reaction completes the catalytic cycle. The active form of the enzyme consists of the tyrosyl radical at Tyr272 coordinated to Cu(II). Coordination of substrate at the site occupied by acetate ion in the X-ray structure (Figure 8a) is followed by deprotonation of the hydroxyl of the substrate by Tyr495. Electron transfer from the alkoxide to Cu(II) (see similarity with first step of TPQ formation, Figure 6) is followed by abstraction of the pro-S hydrogen atom by the tyrosyl radical (step 3). Alternatively, a reversed order of hydrogen atom abstraction and electron transfer has been proposed [77].

Cytochrome c oxidase: a Tyr–His cross-link

Cytochrome c oxidase (CcO), located in the inner membrane of mitochondria or bacteria, catalyzes the four-electron reduction of molecular oxygen to water, an essential step in the respiratory chain (equation 1).

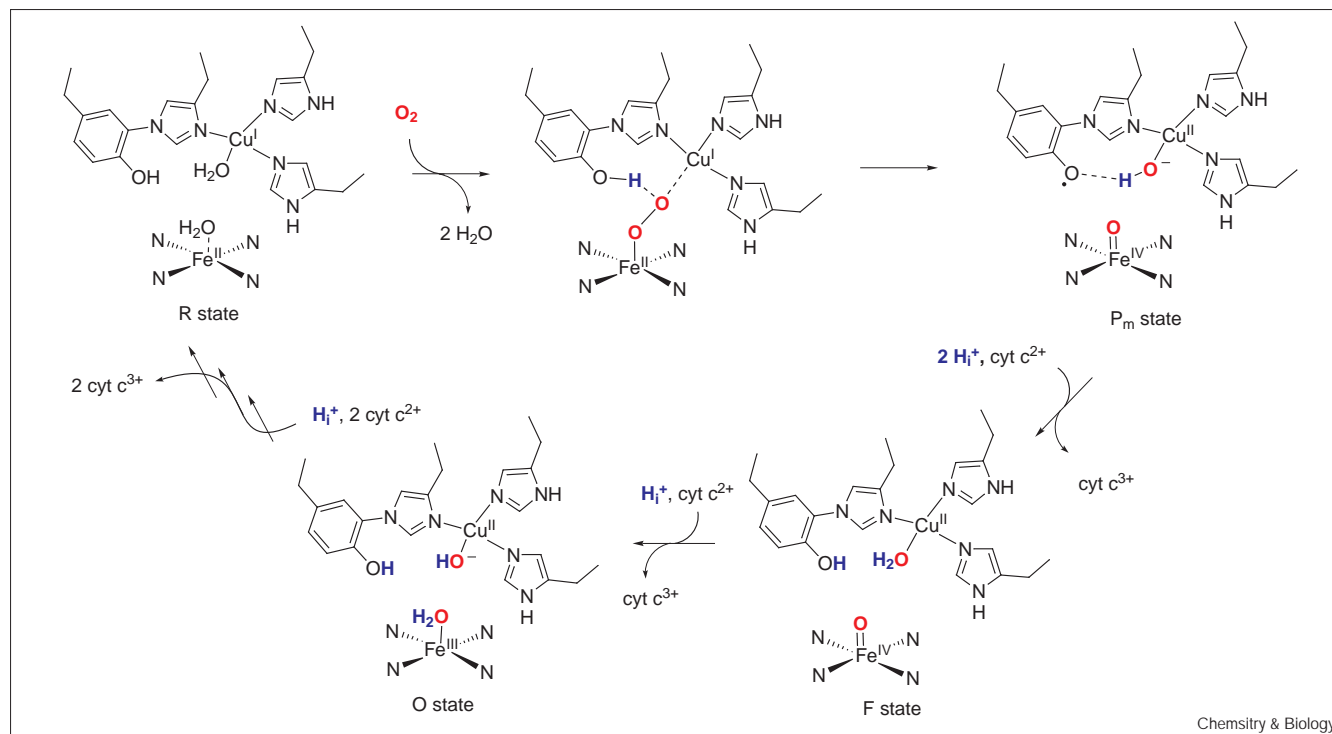


In this process four protons are taken up from the mitochondrial matrix or bacterial cytoplasm (H_i^+) and four electrons are provided by ferrous cytochrome c at the mitochondrial intermembrane space or bacterial periplasm, respectively. Concurrently, four more protons are moved across the membrane (H_o^+) during each turnover, resulting in a total translocation of eight charges [30–32]. The active site of the enzyme contains a binuclear center composed of heme a_3 and Cu_B . Recent crystallographic studies of CcO have revealed a unique and unexpected post-translational modification resulting in a tyrosine cross-linked at C6 to the ϵ -nitrogen of a histidine residue (Figure 8b) [33,34]. Since its discovery, a number of functional roles have been offered for the cross-linked residue. In most proposed mechanisms, the tyrosine, which is located at the end of a possible proton channel to

the surface (K-channel), provides a hydrogen atom to the distal oxygen atom of molecular oxygen bound to the heme during the O–O bond cleaving step (Figure 10) [31,32,35]. In this model, three of the four electrons required for O–O bond breakage are supplied by the metal centers. The mechanistic advantage of using tyrosine as the source of the fourth electron might lie in its ability to transfer an electron and proton simultaneously in the form of a hydrogen atom, thus avoiding the possible formation of highly damaging hydroxyl radical if electron and proton transfer steps were decoupled.

The exact benefits of the presence of a Tyr–His cross-link are only just beginning to be investigated. Studies on model compound 17 (Figure 1) indicate that the cross-link decreases the phenol pK_a by about 1.5 and modestly raises the oxidation potential (~ 60 mV) [36]. A thermochemical cycle based on this data indicates that the O–H bond dissociation energy is not significantly perturbed in stark contrast to the Tyr–Cys cross-link in galactose oxidase (see above). Thus, the cross-link may be ideally suited for its role in turnover: on the one hand, its oxidation potential is kept high, ensuring a strong driving force for the reduction of the radical form in the conversion of the P-state to the

Figure 10



Proposed mechanism for CcO [31,32,35]; proton pumping steps are omitted and the heme is shown schematically. Oxygen reacts with the reduced enzyme to form a heme-bound oxygen species. Subsequent hydrogen atom transfer from Tyr244 to the distal oxygen atom and electron transfer from Cu(I) generates an oxoferryl species and

copper-bound hydroxide. This proposal is consistent with growing evidence that the O–O bond has been cleaved in the P_m state to produce an oxoferryl intermediate [35,78]. Several protonation and electron transfer steps reduce the P_m state back to the R state.

F-state, which drives proton pumping. On the other hand, an increased oxidation potential would unfavorably affect the hydrogen atom abstraction in the A-to-P conversion, but this is compensated for by a decreased pK_a , leading to an effectively unchanged BDE. Similar studies in which 17 or a related structure is coordinated to copper are needed to further explore the altered properties of Tyr244 and His240. The presence of a covalent connection between Cu_B and Tyr272 by virtue of His240 might allow resonance stabilization of the tyrosyl radical in the P_m state, perhaps even resulting in some TyrO⁻/Cu(III) character. The X-ray structure, however, suggests that the geometry of the cross-link is not optimal for such stabilization, as the planes of the tyrosine ring and the imidazole are not coplanar (45°).

In addition to its involvement in O–O bond cleavage, the cross-link might have other roles. Yoshikawa [33] suggested that the pK_a of the modified tyrosine could be sufficiently depressed for it to be deprotonated in the fully oxidized state of the enzyme. Thus, protonation of Tyr244 would be required to prime the enzyme for catalysis and as such might serve a regulatory role. Indeed, in the reductive half of the catalytic cycle, the fully oxidized enzyme (O-state) has been reported to take up two protons as well as two electrons to reduce the binuclear site to its Fe²⁺/Cu⁺ oxidation state (R state). It has been proposed that these protons are delivered to the binuclear center via Tyr244, and that one of the protons is used to protonate Tyr244 to prepare it for its role in O–O cleavage [31]. Proton uptake is complicated, however, by uncertainty about which steps in the CcO catalytic cycle are coupled to proton pumping across the membrane, presently a topic of much debate [32,37]. In summary, although our understanding of the mechanism of catalysis by CcO has enormously improved in the past three years, the exact role of the cross-link, as well as its mechanism of formation, need to be examined further in the future.

Tyr–His and His–Cys cross-links: catalase, tyrosinase, hemocyanin and catechol oxidase

Two other unusual cross-links involving histidine have been reported (Figure 1). The crystal structure of catalase HPII from *E. coli* revealed a covalent bond between N δ of His392 and C β of Tyr415, the proximal heme ligand (4, Figure 1) [38]. This modification was confirmed using mass spectrometry of a tryptic peptide mixture. In about two thirds of the digestion mixture the Tyr415-containing peptide was no longer linked to the His392-containing peptide, suggesting that this linkage might be labile under the conditions used. Interestingly, the modification was only found in subunits in which heme *b* had been converted to heme *d*, suggesting that this previously known autocatalytic conversion might be coupled to the His–Tyr bond formation. The stereochemistry at the β carbon in 4, which was not specified in the original report, is *R* (I. Fita,

and J. Loewen, personal communication). Mutants in which His392 had been replaced did not show any catalytic activity, but this residue is not conserved in catalases suggesting that it is not essential in all members of this family. Catalase from *Proteus mirabilis* contains a different post-translational modification in the form of a methionine sulfone located at position 53 on the distal side of its heme, as observed in crystallographic studies [39]. This residue is also not conserved and a valine is usually found at this position. For both modifications, neither the mechanism of formation nor their functional roles are presently known.

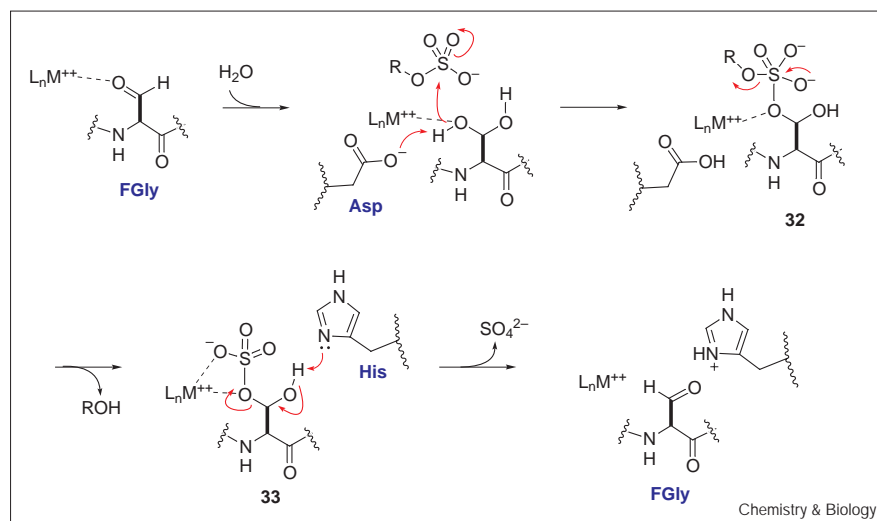
Covalent attachment of cysteine to C ϵ of histidine is found in tyrosinase [40], hemocyanin [41] and catechol oxidase [42]. The X-ray structures for the latter two enzymes [42,43], as well as amino acid sequencing, mass spectrometric analysis of peptic and tryptic peptides and chemical derivatization studies for tyrosinase [40], are consistent with 5 as the structure of the modification (Figure 1). The histidines involved are ligands to one of the copper atoms in the active-site dinuclear center in these proteins, suggesting that the cross-link might play a role in catalysis. The mechanism of formation of the covalent linkage and its exact function remain to be established.

Sulfatases: conversion of serine to formylglycine

Sulfatases catalyze the hydrolysis of a plethora of sulfate esters, ranging from polysaccharides to glycolipids and hydroxysteroids. In humans, deficiencies in specific sulfatases can lead to clinical disorders, including the rare lysosomal storage disorder multiple sulfatase deficiency (MSD). The presence of a post-translational modification had been suspected on the basis of genetic complementation studies, as well as experiments in which sulfatases expressed in MSD fibroblasts failed to generate catalytically active polypeptides. In 1995, Schmidt *et al.* [44] demonstrated that a conserved cysteine residue is converted into 2-amino-3-oxopropionic acid (formylglycine, FGly). So far, this modification is conserved among human sulfatases as well as in the prokaryote *Klebsiella pneumoniae* [45] (the latter involves the conversion of a serine to formylglycine). In the MSD fibroblast inactive proteins, this modification had not occurred. Recently, the structures of human arylsulfatases A and B (ASA and ASB) have been reported [46,47]. Both contained hydrated aldehyde functionalities at the former cysteine site, and showed the presence of a previously undetected metal ion, Ca²⁺ in ASB and Mg²⁺ for ASA. In the ASB structure the hydrated residue was present as a sulfate ester.

Two mechanisms have been proposed for sulfatase catalysis. Both involve a sulfated acetal intermediate 33, but they differ in the mechanism of its formation. In the original model, the sulfate of the substrate attacks the aldehyde [46], followed by displacement of the alcohol by

Figure 11



One of the proposed mechanisms for arylsulfatase [47]. One of the hydroxyl groups of the hydrated formylglycine attacks the sulfate of the substrate displacing an alcohol. The second hydroxyl of the sulfate ester of the hemiacetal 33 facilitates elimination of the sulfate group, regenerating formylglycine. It has been postulated that an aspartate (Asp281 in ASA, Asp300 in ASB) may be involved in initial deprotonation of the acetal aiding in the nucleophilic attack, and that a histidine (His125 in ASA, His147 in ASB) deprotonates the hydroxyl group of the sulfated FGly residue to eliminate sulfate [79].

water, whereas in the second, more recent proposal one of the acetal oxygens adds to the sulfate to generate a 5-coordinate intermediate stabilized by the metal ion (32) [47] (Figure 11). Collapse of the intermediate would release the substrate alcohol and produce the sulfated acetal 33 on the enzyme, which can eliminate sulfate to regenerate formylglycine. The mechanism of oxidation of cysteine or serine to generate the formylglycine cofactor is less well understood. The transformation is known to occur in the endoplasmic reticulum in eukaryotes at a late stage of protein translocation when the protein is still in its unfolded state [48]. Modification is directed by a short sequence beginning with the cysteine to be modified (CTPSR). This short motif (residues 58–73 in ASA) could be inserted into a heterologous peptide and formylglycine formation could be detected at low levels. When seven additional residues from the sulfatase sequence were added (residues 74–80) the efficiency of formylglycine formation approached control values [49]. The identity of the modifying machinery is still unknown, but a recent study has illustrated that for the *Klebsiella* sulfatase, an iron sulfur protein AtsB plays a role in the post-translational modification [50], providing an avenue for investigating the mechanism of formylglycine generation.

Phenylalanine ammonia lyase/histidine ammonia lyase (histidase)

Histidine ammonia lyase (HAL) and phenylalanine ammonia lyase (PAL) are involved in the non-oxidative deamination of L-histidine and L-phenylalanine to urocanic and cinnamic acid, respectively. For many decades it was believed that a dehydroalanine residue or a derivative thereof was present as a reactive cofactor. Serine was identified as the modified amino acid by site-directed mutagenesis and by analysis of inactivated enzyme products in both

HAL and PAL from various sources [51–53]. Recently, the X-ray crystal structure of histidine ammonia lyase from *Pseudomonas putida* revealed the presence of 4-methylideneimidazole-5-one (MIO, Figure 1) [54]. The formation of this species is postulated to be an autocatalytic cyclization of Ala142 and Gly144, followed by dehydration of Ser143 (Figure 12a). This process is reminiscent of the autocatalytic formation of the chromophoric cross-link in green fluorescent protein (GFP) from *Aequorea victoria* [55] (Figure 12b).

The mechanism of deamination had been a long-standing problem as the acidity of the β proton is too low for a conventional elimination. Rétey [56] suggested a novel mechanism involving electrophilic attack of the suspected dehydroalanine on either the imidazole (HAL) or the phenyl group (PAL) of the substrate. In this mechanism, the loss of aromaticity especially in phenylalanine (i.e. 34 in Figure 12c) appeared troublesome, but the elucidation of the MIO structure suggests the loss of aromaticity in the substrate might be compensated by the concomitant aromatization of the cofactor.

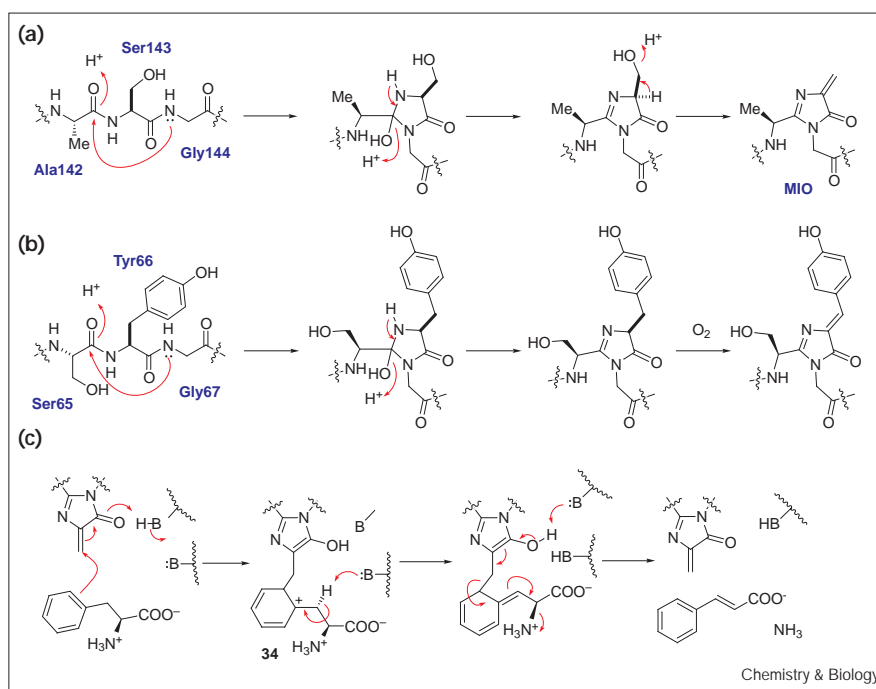
Post-translational modification of metal ligands

Carbamylation of lysine residues: rubisco, urease and phosphotriesterase

A number of proteins have metal ligands that are post-translationally modified. Perhaps the longest known member of this group is ribulose-1,5-bisphosphate carboxylase (rubisco). The enzyme catalyzes the first step in photosynthetic fixation of CO_2 , the carboxylation of ribulose 1,5-bisphosphate (RuBP) to form two molecules of 3-phosphoglycerate, and is responsible for an estimated 10^{11} tons of CO_2 fixation per year. Activated rubisco contains a carbamylated lysine residue that serves as a ligand for an essential Mg^{2+} [57] (6, Figure 1). On the basis of the

Figure 12

(a) The formation of MIO is postulated to be an autocatalytic intrachain cyclization of Ala142 and Gly144, followed by dehydration of Ser143 [54]. (b) In green fluorescent protein, a similar condensation between the amide nitrogen of Gly67 with the carbonyl of Ser65 is followed by autoxidation of the α - β bond of Tyr66 [55]. (c) Proposed mechanisms for PAL. The MIO moiety has enhanced electrophilic character compared to a dehydroalanine. Electrophilic attack of the dehydroalanine of MIO on the phenyl ring of the substrate generates intermediate 34. The acidity of the β protons in this species is significantly increased, facilitating deprotonation. Subsequent base catalyzed elimination of ammonia generates the product. A similar mechanism is proposed for the reaction of histidine with HAL, involving electrophilic attack on the imidazole ring of histidine [54].



X-ray structure of the enzyme complexed with its substrate [58], a detailed mechanism has been proposed that includes a role for the carbamylated lysine as an acid–base catalyst. The carbamylation of the lysine is a reversible and spontaneous process that is prevented when RuBP is tightly bound in the active site. The auxiliary protein rubisco activase is required to remove the inhibitor [59]. Carbamylation of lysine residues is also found in urease [60] and phosphotriesterase [61]. In both proteins the carbamate functions as a bridging ligand between two metal ions, Ni²⁺ in urease, and Zn²⁺ in phosphotriesterase, and as in rubisco, carbamylation occurs readily but the metals are required to stabilize the carbamate. The carbamate, however, is not essential for catalysis in both proteins as additives such as formate and acetate can restore activity in lysine mutants [62,63]. The modification therefore has a primarily structural role.

Nitrile hydratase, NADH peroxidase, peroxiredoxins: conversion of cysteine to cysteine sulfenic acid

A different post-translational modification of metal ligands is found in nitrile hydratase. This non-heme iron-dependent enzyme catalyzes the hydration of nitriles to amides and has been used in the industrial production of acrylamide and nicotinamide [64]. The enzyme is inactive in the dark because of a persistent tightly associated nitric oxide molecule that coordinates to the iron. Irradiation activates the protein by photodissociation of the NO, which is probably replaced with a hydroxide ligand that participates in catalysis. In the X-ray structure of NO-inactivated enzyme two cysteine ligands are present as a sulfenic acid 7 and a

sulfenic acid 8 [65]. These modifications were also present in tryptic peptides as determined using mass spectrometry. Neither the mechanism of oxidation nor the functional roles of the oxidized cysteines are presently known. Cysteine sulfenic acids are also believed to be involved in the redox regulation of several transcription factors including Fos and Jun, and have been reported as catalytically active redox cofactors in peroxiredoxins and the flavoproteins NADH peroxidase and NADH oxidase from gram-positive enteric streptococci (for a review see [66]). These bacteria are unable to biosynthesize heme, and therefore lack catalase. Instead the flavoproteins NADH peroxidase and NADH oxidase reduce H₂O₂ and O₂, respectively, in these organisms. A crystal structure of the NADH peroxidase has confirmed the presence of a sulfenic acid at a position that is occupied by a disulfide in members of the disulfide reductase family with which the peroxidase shares significant homology [67]. This position supports the proposed role of the sulfenic acid as a redox cofactor. The stability of cysteine sulfenic acids in all these proteins is remarkable given its high reactivity in solution [66].

Methyl CoM reductase

Methyl-coenzyme M reductase catalyzes the final step in the formation of methane in methanogenic bacteria. The structure elucidation of the enzyme from *Methanobacterium thermoautotrophicum* revealed the existence of five modified amino acids at or near the active site region [68]. These residues include four methylated amino acids, 5-(*S*)-methylarginine (9), 2-(*S*)-methylglutamine (10),

S-methylcysteine (12), *N*^δ-methyl-histidine (13), as well as thioglycine (11). Their existence has since been confirmed by mass spectrometry of chymotryptic peptides by Thauer and coworkers [69]. The modified residues are 100% conserved among 12 different methanogenic bacteria with different growth temperature optima and phylogenetic origin, and the post-translationally introduced methyl groups are derived from *S*-adenosylmethionine [69]; their structural and/or mechanistic roles remain to be established. The origin of the fifth modified amino acid, thioglycine, is at present unclear. It has been suggested that it might serve as a one-electron redox cofactor forming a thioketyl radical anion during catalysis [70].

Summary and outlook

This review has focused on cofactors that are post-translationally derived from encoded amino acids. With the exception of the proteins that contain a chemically reactive group (His decarboxylase, the quinoproteins, HAL and PAL, and sulfatase), for which modified structures were anticipated on the basis of biochemical studies, these modifications were unexpected. Tyrosine residues are involved in half of the proteins discussed here and appear to be most extensively used in nature to generate proteinaceous cofactors. Although the function and biogenesis of some of the modifications is well understood, others will be subject to future investigation. It is clear that given the frequency of discovery of post-translationally modified active sites, many more are yet to be revealed. In the past decade, X-ray crystallography has been the major tool for detection of spectroscopically and chemically 'silent' modifications. In the near future, however, modern mass spectrometry with its adaptability to high-throughput screening will probably play a major role in the discovery of novel post-translationally generated cofactors [71].

Acknowledgements

Research on post-translational modifications in the laboratory of W.A.V. is supported by the National Institutes of Health (GM5882) and the Burroughs-Wellcome Fund (APP 1920). N.M.O. gratefully acknowledges a predoctoral fellowship from Abbott Laboratories.

References

- van Poelje, P.D. & Snell, E.E. (1990). Pyruvoyl-dependent enzymes. *Annu. Rev. Biochem.* 59, 29-59.
- Kabisch, U.C., Gräntzdörffer, A., Schierhorn, A., Rücknagel, K.P., Andreesen, J.R. & Pich, A. (1999). Identification of D-proline reductase from *Clostridium sticklandii* as a selenoenzyme and indications for a catalytically active pyruvoyl group derived from a cysteine residue by cleavage of a proprotein. *J. Biol. Chem.* 274, 8445-8454.
- Wagner, M., Sonntag, D., Grimm, R., Pich, A. & Eckerskorn, C. (1999). Substrate-specific selenoprotein B of glycine reductase from *Eubacterium acidaminophilum* - biochemical and molecular analysis. *Eur. J. Biochem.* 260, 38-49.
- Klinman, J.P. & Mu, D. (1994). Quinoenzymes in biology. *Annu. Rev. Biochem.* 63, 299-344.
- Janes, S.M., et al., & Klinman, J.P. (1990). A new redox cofactor in eukaryotic enzymes: 6-hydroxydopa at the active site of bovine serum amine oxidase. *Science* 248, 981-987.
- McIntire, W.S., Wemmer, D.E., Chistoserdov, A. & Lidstrom, M.E. (1991). A new cofactor in a prokaryotic enzyme: tryptophan tryptophylquinone as the redox prosthetic group in methylamine dehydrogenase. *Science* 252, 817-824.
- Wang, S.X., et al., & Klinman, J.P. (1996). A crosslinked cofactor in lysyl oxidase: redox function for amino acid side chains. *Science* 273, 1078-1084.
- Wilmot, C.M., et al., & Phillips, S.E. (1997). Catalytic mechanism of the quinoenzyme amine oxidase from *Escherichia coli*: exploring the reductive half-reaction. *Biochemistry* 36, 1608-1620.
- Wilce, M.C., et al., & Yamaguchi, H. (1997). Crystal structures of the copper-containing amine oxidase from *Arthrobacter globiformis* in the holo and apo forms: implications for the biogenesis of topaquinone. *Biochemistry* 36, 16116-16133.
- Li, R., Klinman, J.P. & Mathews, F.S. (1998). Copper amine oxidase from *Hansenula polymorpha*: the crystal structure determined at 2.4 Å resolution reveals the active conformation. *Structure* 6, 293-307.
- Chen, L., et al., & Hol, W.G.J. (1991). Crystallographic investigations of the tryptophan-derived cofactor in the quinoprotein methylamine dehydrogenase. *FEBS Lett.* 287, 163-166.
- Su, Q. & Klinman, J.P. (1998). Probing the mechanism of proton coupled electron transfer to dioxygen: the oxidative half-reaction of bovine serum amine oxidase. *Biochemistry* 37, 12513-12525.
- Mure, M. & Klinman, J.P. (1995). Model studies of topaquinone-dependent amine oxidases. 1. Oxidation of benzylamine by topaquinone analogs. *J. Am. Chem. Soc.* 117, 8698-8706.
- Agostinelli, E., De Matteis, G., Mondovì, B. & Morpurgo, L. (1998). Reconstitution of Cu²⁺-depleted bovine serum amine oxidase with Co²⁺. *Biochem. J.* 330, 383-387.
- Wilmot, C.M., Hajdu, J., McPherson, M.J., Knowles, P.F. & Phillips, S.E. (1999). Visualization of dioxygen bound to copper during enzyme catalysis. *Science* 286, 1724-1728.
- Matsuzaki, R., Fukui, T., Sato, H., Ozaki, Y. & Tanizawa, K. (1994). Generation of the topa quinone cofactor in bacterial monoamine oxidase by cupric ion-dependent autooxidation of a specific tyrosyl residue. *FEBS Lett.* 351, 360-364.
- Cai, D. & Klinman, J.P. (1994). Evidence of a self-catalytic mechanism of 2,4,5-trihydroxyphenylalanine quinone biogenesis in yeast copper amine oxidase. *J. Biol. Chem.* 269, 32039-32042.
- Ruggiero, C.E. & Dooley, D.M. (1999). Stoichiometry of the topa quinone biogenesis reaction in copper amine oxidases. *Biochemistry* 38, 2892-2898.
- Dooley, D.M. (1999). Structure and biogenesis of topaquinone and related cofactors. *J. Biol. Inorg. Chem.* 4, 1-11.
- Dove, J.E., Smith, A.J., Kuchar, J., Brown, D.E., Dooley, D.M. & Klinman, J.P. (1996). Identification of the quinone cofactor in a lysyl oxidase from *Pichia pastoris*. *FEBS Lett.* 398, 231-234.
- Frebort, I., et al., & Adachi, O. (1996). Two amine oxidases from *Aspergillus niger* AKU 3302 contain topa quinone as the cofactor: unusual cofactor link to the glutamyl residue occurs only at one of the enzymes. *Biochim. Biophys. Acta* 1295, 59-72.
- Chen, L., Durley, R.C., Mathews, F.S. & Davidson, V.L. (1994). Structure of an electron transfer complex: methylamine dehydrogenase, amicyanin, and cytochrome c551i. *Science* 264, 86-90.
- Stubbe, J. & van der Donk, W.A. (1998). Protein radicals in enzyme catalysis. *Chem. Rev.* 98, 705-762.
- Whittaker, J.W. & Whittaker, M.M. (1998). Radical copper oxidases, one electron at a time. *Pure Appl. Chem.* 70, 903-910.
- Whittaker, M.M. & Whittaker, J.W. (1988). The active site of galactose oxidase. *J. Biol. Chem.* 263, 6074-6080.
- Whittaker, M.M. & Whittaker, J.W. (1990). A tyrosine-derived free radical in apogalactose oxidase. *J. Biol. Chem.* 265, 9610-9613.
- Ito, N., et al., & Knowles, P.F. (1991). Novel thioether bond revealed by a 1.7 Å crystal structure of galactose oxidase. *Nature* 350, 87-90.
- Johnson, J.M., Halsall, H.B. & Heineman, W.R. (1985). Redox activation of galactose oxidase: thin layer electrochemical study. *Biochemistry* 24, 1579-1585.
- Itoh, S., et al., & Fukuzumi, S. (1997). Active site models for galactose oxidase - electronic effect of the thioether group in the novel organic cofactor. *Inorg. Chem.* 36, 1407-1416.
- Ferguson-Miller, S. & Babcock, G.T. (1996). Heme/copper terminal oxidases. *Chem. Rev.* 96, 2889-2907.
- Gennis, R.B. (1998). Multiple proton-conducting pathways in cytochrome oxidase and a proposed role for the active-site tyrosine. *Biochim. Biophys. Acta* 1365, 241-248.
- Michel, H. (1999). Cytochrome c oxidase: catalytic cycle and mechanisms of proton pumping-- a discussion. *Biochemistry* 38, 15129-15140; and reply by Wikstrom, M. *ibid.* (2000) 3515-3519.
- Yoshikawa, S., et al., & Tsukihara, T. (1998). Redox-coupled crystal structural changes in bovine heart cytochrome c oxidase. *Science* 280, 1723-1729.

34. Ostermeier, C., Harrenga, A., Ermler, U. & Michel, H. (1997). Structure at 2.7 Å resolution of the *Paracoccus denitrificans* two-subunit cytochrome c oxidase complexed with an antibody F-V fragment. *Proc. Natl Acad. Sci. USA* 94, 10547-10553.
35. Proshlyakov, D.A., Pressler, M.A. & Babcock, G.T. (1998). Dioxygen activation and bond cleavage by mixed-valence cytochrome c oxidase. *Proc. Natl Acad. Sci. USA* 95, 8020-8025.
36. McCauley, K.M., Vrtis, J.M., Dupont, J. & van der Donk, W.A. (2000). Insights into the functional role of the tyrosine-histidine linkage in cytochrome c oxidase. *J. Am. Chem. Soc.* 122, 2403-2404.
37. Verkhovskiy, M.I., Jasaitis, A., Verkhovskaya, M.L., Morgan, J.E. & Wikstrom, M. (1999). Proton translocation by cytochrome c oxidase. *Nature* 400, 480-483.
38. Bravo, J., et al., & Loewen, P.C. (1997). Identification of a novel bond between a histidine and the essential tyrosine in catalase HPII of *Escherichia coli*. *Protein Sci.* 6, 1016-1023.
39. Buzy, A., et al., & Hudry-Clergeon, G. (1995). Complete amino acid sequence of *Proteus mirabilis* PR catalase. Occurrence of a methionine sulfone in the close proximity of the active site. *J. Protein Chem.* 14, 59-72.
40. Lerch, K. (1982). Primary structure of tyrosinase from *Neurospora crassa*. II. Complete amino acid sequence and chemical structure of a tripeptide containing an unusual thioether. *J. Biol. Chem.* 257, 6414-6419.
41. Gielens, C., De Geest, N., Xin, X.Q., Devreese, B., Van Beeumen, J. & Preaux, G. (1997). Evidence for a cysteine-histidine thioether bridge in functional units of molluscan haemocyanins and location of the disulfide bridges in functional units δ and γ of the β C-haemocyanin of *Helix pomatia*. *Eur. J. Biochem.* 248, 879-888.
42. Klabunde, T., Eicken, C., Sacchettini, J.C. & Krebs, B. (1998). Crystal structure of a plant catechol oxidase containing a dicopper center. *Nat. Struct. Biol.* 5, 1084-1090.
43. Cuff, M.E., Miller, K.I., van Holde, K.E. & Hendrickson, W.A. (1998). Crystal structure of a functional unit from *Octopus hemocyanin*. *J. Mol. Biol.* 278, 855-70.
44. Schmidt, B., Selmer, T., Igendoh, A. & von Figura, K. (1995). A novel amino acid modification in sulfatases that is defective in multiple sulfatase deficiency. *Cell* 82, 271-278.
45. Miech, C., Dierks, T., Selmer, T., von Figura, K. & Schmidt, B. (1998). Arylsulfatase from *Klebsiella pneumoniae* carries a formylglycine generated from a serine. *J. Biol. Chem.* 273, 4835-4837.
46. Bond, C.S., et al., & Guss, J.M. (1997). Structure of a human lysosomal sulfatase. *Structure* 5, 277-289.
47. Lukatela, G., et al., & Saenger, W. (1998). Crystal structure of human arylsulfatase A: the aldehyde function and the metal ion at the active site suggest a novel mechanism for sulfate ester hydrolysis. *Biochemistry* 37, 3654-3664.
48. Dierks, T., Schmidt, B. & von Figura, K. (1997). Conversion of cysteine to formylglycine: a protein modification in the endoplasmic reticulum. *Proc. Natl Acad. Sci. USA* 94, 11963-11968.
49. Dierks, T., Lecca, M.R., Schlotterhose, P., Schmidt, B. & von Figura, K. (1999). Sequence determinants directing conversion of cysteine to formylglycine in eukaryotic sulfatases. *EMBO J.* 18, 2084-2091.
50. Szameit, C., Miech, C., Balleininger, M., Schmidt, B., von Figura, K. & Dierks, T. (1999). The iron sulfur protein AtsB is required for posttranslational formation of formylglycine in the *Klebsiella* sulfatase. *J. Biol. Chem.* 274, 15375-15381.
51. Hernandez, D., Stroh, J.G. & Phillips, A.T. (1993). Identification of Ser143 as the site of modification in the active site of histidine ammonia-lyase. *Arch. Biochem. Biophys.* 307, 126-132.
52. Taylor, R.G. & McInnes, R.R. (1994). Site-directed mutagenesis of conserved serines in rat histidase. Identification of serine 254 as an essential active site residue. *J. Biol. Chem.* 269, 27473-27477.
53. Schuster, B. & Rétey, J. (1994). Serine-202 is the putative precursor of the active site dehydroalanine of phenylalanine ammonia lyase. Site-directed mutagenesis studies on the enzyme from parsley (*Petroselinum crispum* L.). *FEBS Lett.* 349, 252-254.
54. Schwede, T.F., Rétey, J. & Schulz, G.E. (1999). Crystal structure of histidine ammonia-lyase revealing a novel polypeptide modification as the catalytic electrophile. *Biochemistry* 38, 5355-5361.
55. Heim, R., Prasher, D.C. & Tsien, R.Y. (1994). Wavelength mutations and posttranslational autooxidation of green fluorescent protein. *Proc. Natl Acad. Sci. USA* 91, 12501-12504.
56. Rétey, J. (1996). Enzymatic catalysis by Friedel-Crafts-type reactions. *Naturwissenschaften* 83, 439-447.
57. Cleland, W.W., Andrews, T.J., Gutteridge, S., Hartman, F.C. & Lorimer, G.H. (1998). Mechanism of rubisco – the carbamate as general base. *Chem. Rev.* 98, 549-561.
58. Taylor, T.C. & Andersson, I. (1997). The structure of the complex between rubisco and its natural substrate ribulose 1,5-bisphosphate. *J. Mol. Biol.* 265, 432-444.
59. Portis, A.R., Jr. (1990). Rubisco activase. *Biochim. Biophys. Acta* 1015, 15-28.
60. Jabri, E., Carr, M.B., Hausinger, R.P. & Karplus, P.A. (1995). The crystal structure of urease from *Klebsiella aerogenes*. *Science* 268, 998-1004.
61. Benning, M.M., Kuo, J.M., Raushel, F.M. & Holden, H.M. (1995). Three-dimensional structure of the binuclear metal center of phosphotriesterase. *Biochemistry* 34, 7973-7978.
62. Kuo, J.M., Chae, M.Y. & Raushel, F.M. (1997). Perturbations to the active site of phosphotriesterase. *Biochemistry* 36, 1982-1988.
63. Pearson, M.A., Schaller, R.A., Michel, L.O., Karplus, P.A. & Hausinger, R.P. (1998). Chemical rescue of *Klebsiella aerogenes* urease variants lacking the carbamylated-lysine nickel ligand. *Biochemistry* 37, 6214-6220.
64. Kobayashi, M. & Shimizu, S. (1998). Metalloenzyme nitrile hydratase: structure, regulation, and application to biotechnology. *Nat. Biotechnol.* 16, 733-736.
65. Nagashima, S., et al., & Endo, I. (1998). Novel non-heme iron center of nitrile hydratase with a claw setting of oxygen atoms. *Nat. Struct. Biol.* 5, 347-351.
66. Claiborne, A., et al., & Parsonage, D. (1999). Protein-sulfenic acids: diverse roles for an unlikely player in enzyme catalysis and redox regulation. *Biochemistry* 38, 15407-16.
67. Yeh, J.I., Claiborne, A., Hol, W.G. (1996). Structure of the native cysteine-sulfenic acid redox center of enterococcal NADH peroxidase refined at 2.8 Å resolution. *Biochemistry* 35, 9951-7.
68. Ermler, U., Grabarse, W., Shima, S., Goubeaud, M. & Thauer, R.K. (1997). Crystal structure of methyl coenzyme M reductase - the key enzyme of biological methanogenesis. *Science* 278, 1457-1462.
69. Selmer, T., et al., & Thauer, R.K. (2000). The biosynthesis of methylated amino acids in the active site region of methyl-coenzyme M reductase. *J. Biol. Chem.* 275, 3755-3760.
70. Thauer, R.K. (1998). Biochemistry of methanogenesis - a tribute to Stephenson, Marjory. *Microbiology* 144, 2377-2406.
71. Kelleher, N.L. (2000). From primary structure to function: biological insights from large-molecule mass spectra. *Chem. Biol.* 7, R37-R45.
72. Gallagher, T., Rozwarski, D.A., Ernst, S.R. & Hackert, M.L. (1993). Refined structure of the pyruvoyl-dependent histidine decarboxylase from *Lactobacillus* 30a. *J. Mol. Biol.* 230, 516-528.
73. Dooley, D.M., McGuire, M.A., Brown, D.E., Turowski, P.N., McIntire, W.S. & Knowles, P.F. (1991). A Cu(II)-semiquinone state in substrate-reduced amine oxidases. *Nature* 349, 262-264.
74. Medda, R., Padiglia, A., Bellelli, A., Pedersen, J.Z., Agro, A.F. & Floris, G. (1999). Cu(II)-semiquinone radical species in plant copper-amine oxidases. *FEBS Lett.* 453, 1-5.
75. Chen, L., et al., & Mathews, F.S. (1998). Refined crystal structure of methylamine dehydrogenase from *Paracoccus denitrificans* at 1.75 Å resolution. *J. Mol. Biol.* 276, 131-149.
76. Zhu, Z. & Davidson, V.L. (1999). Identification of a new reaction intermediate in the oxidation of methylamine dehydrogenase by amicyanin. *Biochemistry* 38, 4862-4867.
77. Wachter, R.M. & Branchaud, B.P. (1998). Construction and analysis of a semi-quantitative energy profile for the reaction catalyzed by the radical enzyme galactose oxidase. *Biochim. Biophys. Acta* 1384, 43-54.
78. Fabian, M., Wong, W.W., Gennis, R.B. & Palmer, G. (1999). Mass spectrometric determination of dioxygen bond splitting in the "peroxy" intermediate of cytochrome c oxidase. *Proc. Natl Acad. Sci. USA* 96, 13114-13117.
79. Waldow, A., Schmidt, B., Dierks, T., von Bülow, R. & von Figura, K. (1999). Amino acid residues forming the active site of arylsulfatase A: role in catalytic activity and substrate binding. *J. Biol. Chem.* 274, 12284-12288.